Optimisation of Fluid Mixing in a Hydrosac© Growing Module

Problem presented by

Adam Dixon and Thanya Charts. (Phytoponics)

ESGI138 was jointly hosted by
The University of Bath
The University of Bristol

Report Authors and Contributors

Facilitator: Alan Champneys (University of Bristol)
Contributors: Graham Benham, (University of Oxford), Stephen Cowley (University of Cambridge), Zoe Dennison (University of Bath), Matthew Griffith (University of Bath), Alissa Kamilova (University of Oxford), Attila Kovács (University of Oxford), Andrew Lacey (Heriot-Watt University), Scott Marquis (University of Oxford), Piotr Morawiecki (Polish Academy of Sciences), John Ockendon (University of Oxford), Rahil Sachak-Patwa (University of Oxford), Colin Please (University of Oxford), Hayley Wragg (University of Bath).

Contents

1   Executive Summary

A mathematical model is sought for the flow of nutrients in the Hydrosac© growing module being developed by Phytoponics. The basic operation involves long fluid-filled bags with periodic growing zones from which root systems emerge into the bulk fluid. The system is periodically perturbed via two main processes: partial drainage and refilling of each bag with nutrient infused water, with inlet and outlet at opposite ends of the bag; and a more violent oxygenation of the water through bubbles that rise from the pores of an aeration tube that runs underneath the central long axis of the bag.

The aim of the modelling is to determine the key parameters and fluid regimes underlying the nutrient mixing process, to ensure that required nutrient levels are maintained throughout the root zones, and to enable optimal scheduling of the nutrient and bubble flow.

Simple experiments were performed via the injection of dye into an operating Hydrosac© that contained semi-mature plants. This enabled a basic understanding of the time and lengthscales of nutrient flow, and also the extent to which mixing occurs in different zones within the bag. Four different flow regimes are identified. At the scale of a single root, a Stokes-flow approximation may be used. At the scale of the individual plant, a so-called Brinkman flow regime may be employed which is describes a transition between slow porous-medium flow and fast channel flow. These equations may be homogenised into a 1D model that can be used to estimate the macro-scale flow of nutrients along the length of the bag.

A shear flow model is used to predict the extent to which this flow permeates into regions dominated by plant roots. This leads to the requirement to model the bubble-driven flow within a bag cross-section containing a plant. Simplified two-phase flow equations are derived and solved within the software COMSOL. The results suggest that the bubble flow is sufficient to drive recirculating flow, which is also found to be consistent with previous literature.

The overall conclusion is that both the periodic flow of nutrients and the aeration are required in order to enable even nutrient spread in the Hydrosac© . Wave effects can be ignored, as can the effect of stagnated nutrient diffusion. The longitudinal nutrient flow enables the whole sack to be reached on the time scale of several cycles of the main inlet flow, while the recirculation from the bubble flow enables enables nutrients to spread within the plant roots. Nevertheless, regions of stagnation can occur via this process near any sharp corners of the bag.

It is recommend that the various analyses are combined into a a reduced-order mathematical model that can be used to optimise the dynamic operation of the Hydrosac© , which can also be adaptable to other geometries and growing conditions.

2 Problem statement

Phytoponics is an 'AgTech' start-up based in Wales. Their vision is to innovate the food chain by facilitating the mass adoption of Hydroponic technology, so that a market sustainable agriculture can tackle this century's food, land and water challenges. Hydroponics is the best way to grow fruit and veg, using 10 times less land and water than a traditional field and it aligns with the UN sustainable development goals. Led by the United Nations Young Champion of the Earth for Europe, Adam Dixon, Phytoponics has invented a new type of low cost and versatile growing system that could deliver a huge impact globally.

Watch video: `https://www.youtube.com/watch?v=Y7ReU6dtJNM&t`

Hydroponics involves growing plants in a water-based nutrient solution to induce higher growth rates. However, in a water environment, a significant constraint is the dissolved oxygen levels, as plant roots respire using this dissolved oxygen as their primary source.

Having adequate dissolved oxygen levels is essential for healthy roots due to maintaining pathogen defence systems and nutrient uptake. It is also important that nutrients are well mixed within the system and that natural fluid flow does not cause dead zones or poor concentration gradients within the growing system.

Phytoponics as a start-up has already benefited directly from taking part in two KTN agri-food mini-study-groups with industry in 2017 and 2018. The innovations developed there involved optimising the geometry of the sack to ensure its rigidity and understanding how to aerate the system to achieve desired levels of dissolved oxygen.

The bigger challenge presented here is to optimise the design of the fluid mixing within the Hydrosac© growing modules, such that oxygenation is maximised in the pool of water, and that nutrients are well mixed without any dead zones or unintended concentration gradients.

The timing of the ESGI 138 is ideal because during the Study Group, Phytoponics can include analysis and experiments in an ongoing large-scale trial in Wales. There may also be scope to run experimental tests, live, on the actual apparatus, or even to arrange a day trip to visit the trial site during the study group.

Key mathematical questions to be addressed during the study group include:

1. How does the geometry of the Hydrosac© growing module contribute to the spread of nutrients and oxygen?

2. How do plant roots contribute to mixing/and or stagnation?

Figure 1: The Hydrosac© with young tomato plants

3. Can we make a more precise model of nutrient distribution and oxygenation, backed up by data?

4. Could we run experiments with introduction of die to explain how mixing takes place?

5. Could we create an engineering model from applied mathematics for this scenario?

6. Could one design optimal baffles or make other changes to the geometry to aid mixing, and to generally enhance plant growth and cleaning?

3   The Hydrosac© system

Phytoponics have designed an innovative hydroponic technology device and they aim to use this technology to tackle the challenge of supplying sufficient food with limited land and water resources. Hydroponics is the method of growing plants without soil, instead growing them in a solution of water and nutrients.

This report is based on the configuration of Hydrosac© that was being undertaken in Aberystwyth under greenhouse conditions, running concurrently with the Study Group. At the time of the Study Group the trial was in mid stage with the plants not having quite reached maturity. The trial involved 8 separate Hydrosac© connected to a single pump and aeration system. Nevertheless for the purposes of this study, we will consider the
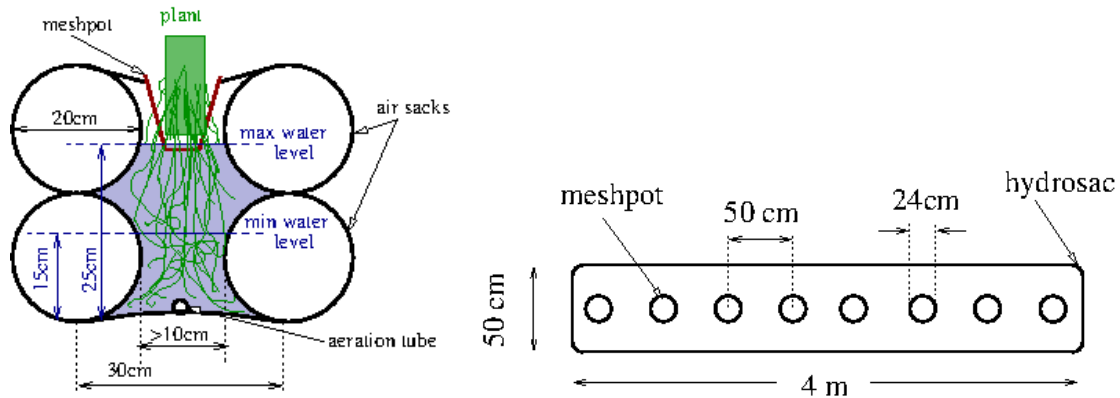
Figure 2: Layout sketch of the Hydrosac© . Left, side view; right, top view
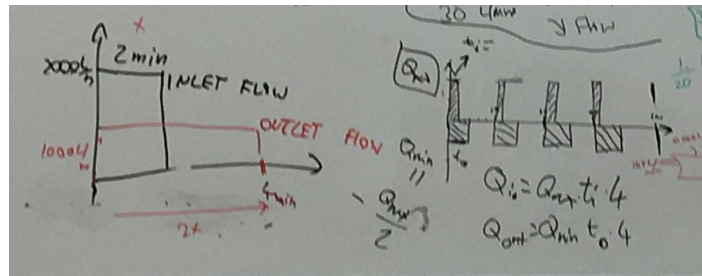
Figure 3: Typical pump and drain schedules during one hour.

situation in a single Hydrosac© rather than the whole system. The basic geometry and dimensions of the Hydrosac© are given in Fig. 2. It can be noted that the double-airbag geometry came about through innovations inspired by the first KTN mini-study-group report [1].

During the Aberystwyth trial, nutrients were provided directly to the root system in each Hydrosac© by a flushing system in which water with freshly dissolved nutrients enters the sack via an inlet in the upper portion of the sack end wall. At the bottom of the far end wall of the sack there is a drain, which can be automatically opened and closed. from which fluid can egress. The drained fluid is pumped through a cleaning system that removes pathogens and dead plant material, before being recycled to have fresh nutrients added and enter through the inlet again. The mass flow rate of the inlet pump is $Q \approx 15\text{L/min}$, whereas that of the drain is $Q/2$. A repeated T_1-periodic cycle is maintained in which both the pump and the inlet are on for a fixed time T_{on}. The mass flow rate of the inlet is During this time the free surface of the water in the sack rises to its maximum level w_{max}. Then, for the same period of time T_{on}, the pump continues to operate. During this time the water-level sinks to its minimum level w_{min}. Then for a further period of time $T_1 - 2T_{\text{on}} > 0$ both the inlet and drain are closed and the water level remains at w_{min}; see fig. 3.

Figure 4: The bubble flow from the aeration tube

During the study group, an additional system of nutrient inflow was being trialed via a sequence of drippers, one for each plant meshpot, which dripped nutrients from above at an estimated rate of $0.066 \mathrm{L/min}$, for about 2 minutes per 15 minutes. Initial computations below will suggest that this method of nutrient input has negligible effect compared with the main input flow. It transpired that, after the study group, the drippers were removed from the trial system.

On a separate cycle, of period T_2, air bubbles are briefly pumped into the bottom of the Hydrosac© for a time $T_a \ll T_2$ through an aeration tube similar to that shown in fig. 4. This meshed tube allows bubble production across the whole surface of the tube, rather than through small holes punctured in its upper surface, as was envisaged in the previous KTN mini-study-group report [2]. This accords with the findings of that report that finer bubbles with a larger total surface area which greatly improve aeration capability.

The trial underway at the time of the study group had $T_1 = T_2 = 15$ min, $T_{\mathrm{on}} = 2$ min and $T_a = 1$ min, so that the entire system cycled every 15 minutes with 1 minute of bubble flow and 6 minutes of flow due to the inlet or drain.

The key question to be addressed is whether with the given geometry and operation schedule, nutrients would be spread evenly around the tank at the required level (about 200 parts per million). Initial measurements from Phytoponics suggested that the nutrient levels could vary within each sack, with sometimes a slightly higher concentration at the drain end and sometimes a higher concentration at the inlet end. This static measurements are however inconclusive, and thus an understanding of the mechanisms that underlie nutrient mixing was sought from the study group.

4   Experimental observations

During the study group, Phytoponics organised several dye experiments so that the flow could be observed and conclusions drawn about its properties. The dye was used to simulate the injection of nutrients into the system.

Two kinds of experiment were performed as follows:

1. Dye is injected at the end of the Hydrosac© . Bubbles are then turned on using the aeration tube. The flow of bubbles is stopped and the main inlet flow is then turned on. Following this the bubbles are then turned on again.

2. Dye is injected at the root base of a plant. The main inlet flow is then turned on. Following this, the bubbles are also turned on.

The full experiment videos are available at:

`https://docs.google.com/presentation/d/1QuAuLZC8Cqv0tY4qe8N_ENtuV6c3rLjYky_2QSQqdpM/edit?usp=sharing`

The following snapshots capture the principal results of the experiments.

4.1   Experiment 1

(a) Bubble flow turned on. No movement of dye observed.

(b) Bubble flow turned off. Main inlet flow turned on. Good movement of dye observed.

(c) Propagation of dye observed further down the Hydrosac© .

(d) Bubble flow again turned on and the solution becomes well mixed.

Figure 5: Pictures illustrating the first experimental procedure.

A summary of the first experimental procedure can be seen in fig. 5. The dye is inserted at the end of the Hydrosac© , and the bubbles are turned on. We observe that no mixing is induced, and the dye remains unmoved. Thus the bubble flow alone is not sufficient to give good mixing.

After this, the main inlet flow is turned on. This results in significant propagation of dye down the Hydrosac© Dye is observed 4 pots away (at least a metre) within a matter of seconds, and it is observed to spread to the whole Hydrosac© within minutes. However, dye remains confined mostly to the root-free region of the flow. In particular there remains very little die along the central axis of the bag, around the plants themselves.

The bubbles are then turned on again. Now that the dye has been well propagated along the axial length of the sack, it was found that the bubbles are now effective in distributing the dye evenly within a cross-section of the sack. In particular, after the bubble flow ceases, there is the appearance of well-mixed solution within the root zone as well as the root-free region of the Hydrosac© .

Thus, it is evident that **both the main inlet flow and bubbles are necessary** to provide a well-mixed solution. It also appeared to be the case that a single **one cycle of each may not be sufficient** when the nutrients are introduced at the end of the Hydrosac© .

4.2   Experiment 2

(a) Main inlet flow turned on. No movement of dye observed.

(b) Bubble flow turned on. Good spread of dye observed.

Figure 6: Pictures illustrating the second experimental procedure.

A summary of the second experimental procedure can be seen in fig. 6. The dye is inserted at the root base of a particular plant and the main inlet flow is turned on. We observe no spread of dye from a region around the roots, and the dye remains relatively unmoved. In this case, the inlet flow alone is not sufficient to spread the dye and provide mixing.

After this, the bubbles are then turned on. This causes significant spread of the dye around the roots and into the surrounding region[1], with the flow then propagating the dye along the axial length of the Hydrosac© . Thus bubbles flow prior to the main inlet flow was necessary to agitate and spread the dye so that it could then be carried by the main flow.

Thus, it is evident that **both the main inlet flow and bubbles are necessary** to provide a flushing of high concentrations of waste products from around the plant roots into the rest of the Hydrosac© . Again we note that a well mixed solution is only obtained after application of the main inlet flow, after the bubble flow. This it seems that the **controlling the timing of bubble flow and inlet flow may be important** in order to maintain a well-mixed solution of nutrients and waste materials.

5   Literature Review and Flow Regimes.

Following the experiments, we conducted a literature review to gain further knowledge on hydroponics, channel flow and bubble mixing, so that we could create a mathematical model to reproduce the observed results. Most of the background literature on hydroponic systems were already known by the Phytoponics team and relevant references were already included in the previous mini-study-group reports [1, 2].

5.1   Bulk flow regime

Many analogous situations could be found to the bulk flow in the bag, for which standard theories could be developed. The key question was to estimate the Reynolds number around the roots. For an inlet rate of

$$15\,\mathrm{L\,min^{-1}} = 2.5 \times 10^{-4}\,\mathrm{m^3\,s^{-1}}$$

and high-water, free-water cross-section of

$$l \times l = 0.2\,\mathrm{m} \times 0.2\,\mathrm{m},$$

---

[1]   It is worth noting that additional dye was added in this step of the experiment and that excess dye was accidentally squirted onto the surface. However, the spread of dye was still attributable to the introduction of the bubbles, as it was seen to quickly spread the injected dye.

the flow speed in free water is of order

$$v = 10^{-2} \, \mathrm{m \, s^{-1}}.$$

This will need significant adjustment for low-water flow when water travels through the root mass.

This gives an estimate of the Reynolds number:

$$Re = \frac{\rho l v}{\mu} \approx \frac{0.2 \, \mathrm{m} \times 10^{-2} \, \mathrm{m \, s^{-1}}}{10^{-3} \times 10^{-3} \, \mathrm{m^2 \, s^{-1}}} = 2 \times 10^3$$

We can also estimate the associated pressure gradient, as the water passes the plants:

$$\nabla p \sim \frac{\rho v^2}{l} = \frac{10^3 \, \mathrm{kg \, m^{-3}} 10^{-4} \, \mathrm{m^2 \, s^{-2}}}{0.2 \, \mathrm{m}} = 0.5 \, \mathrm{Pa \, m^{-1}}$$

With a length scale in the root region of $a = 3 \times 10^{-3}$ m, this pressure gradient would drive a flow speed of order, for Darcy (slow) flow, of order

$$a^2 P_g/\mu \sim 10^{-5} \, \mathrm{m^2} \times 0.5 \, \mathrm{kg \, m^{-2} \, s^{-2}}/(10^{-3} \, \mathrm{kg \, m^{-1} \, s^{-1}}) = 5 \times 10^{-3} \, \mathrm{m \, s^{-1}}.$$

On the the other hand, trying a different Ergun (fast) flow balance, a typical velocity in the root region, v_r, satisfies

$$v_r^2 = a P_g/\rho = 3 \times 10^{-3} \, \mathrm{m} \times 0.5 kg \, \mathrm{m^{-2} \, s^{-2}}/(10^3 \, \mathrm{kg \, m^{-3}}) = 1.5 \times 10^{-6} \, \mathrm{m^2 \, s^{-2}},$$

giving

$$v_r \sim 10^{-3} \, \mathrm{m \, s^{-1}},$$

and a local Reynolds number of

$$\rho v_r a/\mu = 10^3 \times 10^{-3} \times 3 \times 10^{-3}/10^{-3} = 3.$$

These estimates suggest that the flow is borderline between "fast" – Ergun – and "slow" – Darcy. Also the reduced speed is comparable with the earlier speed, just above, for clear water. This would indicate that the use of a Brinkman equation for the flow throughout the sack could be appropriate.

5.2 Mixing due to bubble plumes

A more subtle question for which there is significantly less literature is the how much mixing might be induced by a plume of bubbles.

Bubble plumes are used in mixing reservoirs and lakes. Some examples of bubble mixing models for bubble plumes in large water bodies include Wüest, Norman and Imboden in 1992

[3] they develop a numerical model for a bubble injection plume in a lake and Takashi and Imburger's 1993 model [4] for a linearly stratified environment. However these mixing methods often use the change in temperature to aid the mixing as the bubbles travel differently over this temperature profile. Since the depth in the Phytoponics sack is not big enough to create a significant temperature difference these models were found not to relevant.

The most relevant work we found was in Risso's recent review paper [5] on bubble-induced mixing. He considers an experiment in which gas is released into a stationary liquid without pumping. The fluid is initial stationary, but its geometry ensures a relatively high Reynolds number once the bubble flow begins at $\mathcal{O}(10^3).The experimental observations found that in areas of high bubble concentr$

There are many references to the literature in Risso's paper, containing further details of bubble flow and induced mixing. Other relevant references we found include Ulbrecht and Baykara's paper on liquid phase mixing in a bubble column in [6]. Their paper shows that the viscosity of the fluid significantly influences the quality of mixing from the bubbles. Also Burns and Rice investigated circulation in bubble columns in 1997 [7], showing that the circulating velocity profile is plug shaped not parabolic as predicted previously.

Finally expert input from Stuart Dalziel at the University of Cambridge [8] was solicited. Based on his experimental expertise, he stated that a stream of bubbles can induce convection, provided their rise velocity ga^2/ν is small enough compared with the convective velocities $\sqrt{\phi g L}$, for some typical length scale L and volume concentration ϕ

6   Longitudinal model

If we neglect for now the variation inside a cross section, we can build a one-dimensional model that can be used to evaluate the height changes in a channel for a given inflow and outflow. We start by considering a very simple situation where we assume the flow is slow (Darcy flow) and look at the result longitudinal flow. Then we shall derive equations for the longitudinal flow systematically from a detailed description of the flow everywhere but exploiting the vast range of different lengthscales to simplify the model.

6.1   Longitudinal flow model

We first assume that the flow everywhere is slow and can therefore be taken to be governed by the equations of Darcy flow. The governing equation comes from the conservation of water mass at a given position x along the channel, which can be derived by assuming the flow is unidirectional along the length of the sack and then averaging Darcy's equation in the cross section. This yields a conservation equation for the water cross-sectional area
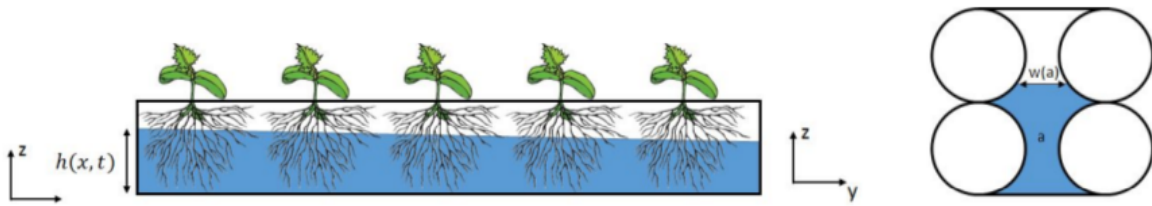
Figure 7: The computational domain

$a(x, t)$ at a given position. For this initial model, we will assume a simple geometry for the sack with a rectangular cross-section of constant width W and height $h(x, t)$, although this can be easily extended to more complex geometries.

The relevant Darcy flow equation is

$$\frac{\partial(\rho W h)}{\partial t} = \frac{\partial}{\partial x} \left[\frac{\kappa \rho g W h}{\mu} \frac{\partial h}{\partial x} \right] + s(x, t), \tag{1}$$

where κ is the permeability of the medium (taking into account the root density), ρ is the water density, g is the gravitational constant, and μ is the viscosity of water. The function s represents mass sources and sinks of water to take into account the various sources of input of water and the root system water uptake. See fig. 8 where the small sources along the length of the sack represent the drippers at each plant. In addition we include the mass input from the inlet sac and the mass removed to the next sack as large sinks and sources at the ends. With this functional form of the source/sink term the boundary conditions for this system are given by no flux, namely

$$\frac{\partial a}{\partial x} = 0 \quad \text{at} \quad x = 0, \tag{2}$$

$$\frac{\partial a}{\partial x} = 0 \quad \text{at} \quad x = L. \tag{3}$$

Finally the initial condition is

$$a = a_0(x) \quad \text{at} \quad t = 0, \tag{4}$$

where a_0 is the initial water height in the sac.

This problem was solved numerically in Mathematica. The solution demonstrated that for given fluxes and typical permeabilities that the variation of height of the free surface at any time instance will be extremely small. There is no evidence of wave effects or sloshing of fluid between the inlet and drain ends of the sack. The water height simply rises and falls at the difference between the total rate of mass input and output.
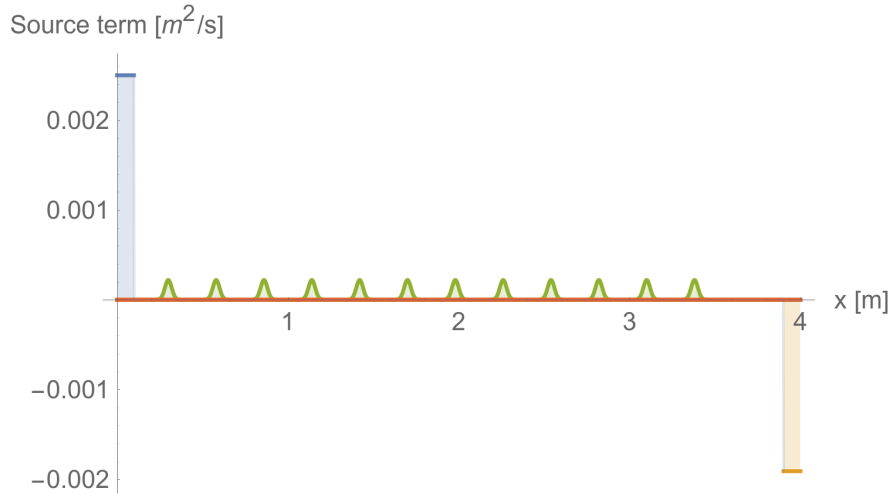
Figure 8: Source terms for the one dimensional model. Blue and orange correspond to the in- and outflow, respectively, green is the dripper effect and brown is the root water uptake.

6.2   Multi-scale model

We shall seek systematically to derive a model of the flow in the sack. We presume that the water can be modelled as a Newtonian viscous fluid and hence the governing equations are the Navier-Stokes equations. We shall need to account of the free surface of the water and the solid boundaries of the Hydrosac© as well as giving some initial data. The geometry of the problem is extremely complex and hence we wish to exploit the many diverse lengthscales in order to derive a simpler set of equations.

In particular, there are three different length scales that we can exploit namely (i) the individual root scale, (ii) the single plant scale (which is also similar to the sack width scale) and (iii) the sack length scale. See Figure 9). The approach taken is to look at the smallest length scale, where we can identify some generic microscale *cell problem* representing a single root. The we use this to upscale to a mesoscale cell problem representing the root ball of a single plant. Finally upscale the mesoscale to produce a macroscopic model on the length scale of the entire sac.

On the microscale, that is the scale of a single plant root, we consider the fluid to be a slow moving, incompressible viscous fluid so that we employ the Stokes equations:

$$-\nabla p + \mu \nabla^2 \mathbf{u} = 0, \tag{5}$$

$$\nabla \cdot \mathbf{u} = 0. \tag{6}$$

Here $\mathbf{u}$ is the velocity of the fluid, μ is the kinematic viscosity and p is the pressure. Treating
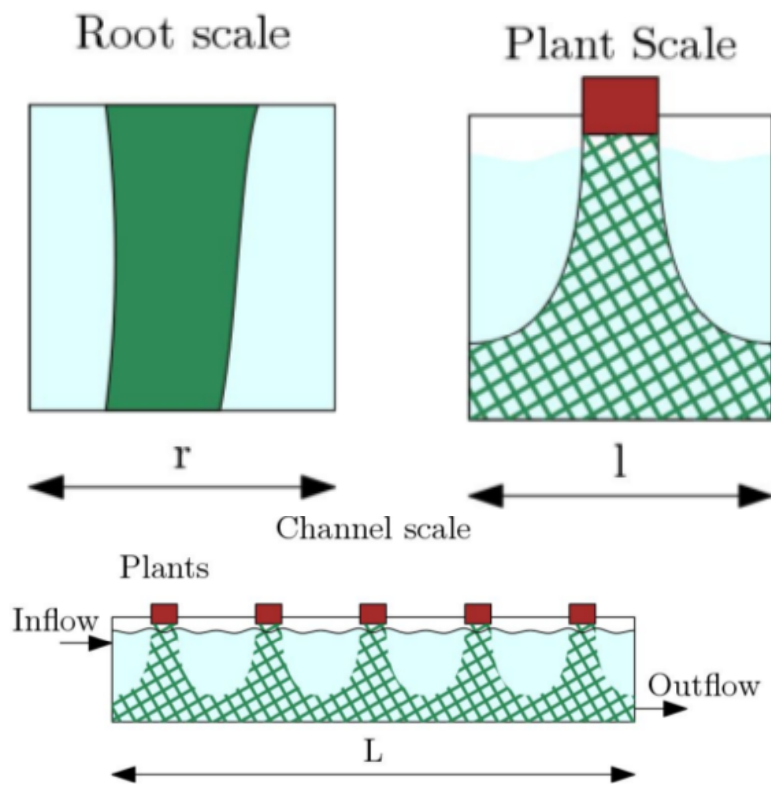
Figure 9: The three length scales of the homogenised model

the fluid in this way is motivated by the low downstream velocities observed in the fluid and the small length scale which give rise to a small Reynolds number.

On the mesoscale, that is the scale of a single plant, we must account for drag associated with the fluid moving past a large mass of roots. We do this by employing a Brinkman flow regime, which can be thought of as Stokes flow with an additional drag term associated with the roots (see e.g. [9], This model is:

$$-\nabla p + \mu \nabla^2 \mathbf{u} - \frac{\mu}{\kappa_1} \mathbf{u} = 0 \tag{7}$$

$$\nabla \cdot \mathbf{u} = 0. \tag{8}$$

Here $\mathbf{u}$ is the fluid velocity, μ the kinematic viscosity, p the pressure, and κ_1 the permeability of the roots. We can can calculate this permeability by solving a 'cell' problem of the flow around a single root in a periodic array of roots with the flow governed by (6).

On the macroscale, that is the scale of the channel, we can homogenise the previous Brinkman flow model for the flow to derive

$$\mathbf{u} + \frac{\kappa_2}{\mu} \nabla p = 0 \tag{9}$$

$$\nabla \cdot \mathbf{u} = 0 \tag{10}$$

which is a Darcy Flow model. Here, $\sqcap$ is the fluid velocity, μ the kinematic viscosity, p the pressure, and κ_2 permeability of the roots on the macroscale. Note that through the homogenisation procedure, one can develop a relationship between κ_2 and the mesoscale geometry and κ_1 by again solving a cell problem of the flow through a collection of roots representing the root ball of a single plant in a periodic line of such plants.

We are also interested in studying how the concentration of nutrients evolves over time in the channel. A realistic situation is that the concentration on the micro and meso scales are nearly spatially uniform and hence at the macroscale we have an advection-diffusion equation for the concentration of nutrients:

$$\frac{\partial c}{\partial t} + \mathbf{u} \cdot \nabla c = D \nabla^2 c - \eta c. \tag{11}$$

Here c is the concentration of nutrient, $\mathbf{u}$ is the fluid velocity at the macroscale, D is the diffusivity of nutrient in water, and η is the rate of absorption of nutrients from the fluid by the plant roots. We enforce fixed a concentration boundary condition on the input of the Hydrosac© , and an outflow condition on the right hand side, given in non-dimensional form by

$$c = 1, \quad x = 0, \tag{12}$$

$$\nabla c \cdot \mathbf{n} = 0 \quad x = 1. \tag{13}$$
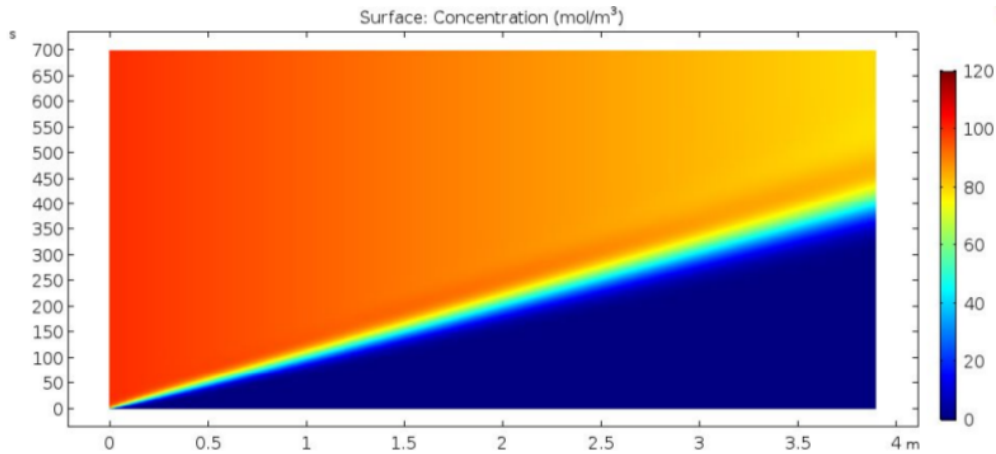
Figure 10: Numerical results from the homogenised model
(vertical axis is time in seconds and horizontal is distance down the sac)

To investigate effects down the whole channel, we first solve (9) and (10) for the channel fluid flow. We set up the three-dimensional cell problem at the mico- and meso-scales. However, due to computational problems in the timescale of the study we were not able to generate solutions of these 'cell' problems. Hence we used an estimated parameter value for k_2. We then use this fluid velocity profile as in input to solve (11). In Figure 10, we plot the concentration profile in the channel as time evolves. We observe a moving front where the nutrients move through the Hydrosac© , being added at the left hand side and flowing out through the right hand side.

We note that it takes 350 seconds which is about 6 minutes for the nutrients to fully advect from the inlet to the drain end of the sack. Note that this is longer than a single time period in which both the inlet and drain are on. This accords with the dye experiment results in which die was not found to spread the whole length of the sack during a single inflow event.

Another conclusion from these results, although not explicitly shown here, is that diffusion alone, will only allow nutrients to spread along the length of the sack over the timescale of hours.

7   Mesoscale models — capturing stagnation and mixing

To investigate the presence of areas of stagnant fluid within the Hydrosac© , we next examine the mesoscale problem. The main assumption we are going to make, in order to make progress, is that the root distribution varies across a cross-section but is uniform along the sac. This will allow us to examine the cross-sectional flow neglecting the fact that the

plants inhomogeneities in the root distribution down the channel between individual plants as well as neglecting height difference along the channel. Hence we will examine flow in a cross-sectional area (with y across the sac and z $vertical$) assuming the flow is unidrectional $u(y,z)$ along the sac. The mesoscale model in the (y,z) plane is therefore

$$\mu \nabla^2 u = \frac{\partial p}{\partial x} + \frac{u}{\kappa(y,z)}, \tag{14}$$

where, μ is the kinematic viscosity, $u(y,z)$ is the unidirectional fluid velocity, and p is the pressure. We close the model by assuming we know the position of the surface and the pressure gradient in the x direction, and taking the boundary conditions to be:

$$u = 0, \quad \text{on the walls of the Hydrosac© ,} \tag{15}$$

$$\frac{\partial u}{\partial n} = 0 \quad \text{on the free surface,} \tag{16}$$

which represents both no penetration of the fluid into the walls of the Hydrosac© and also no slip on the walls of the sac. The second condition represents that there is no flow through the free surface and no shear stress.

In Figure 11, we plot the permeability function across the cross-sectional area; the function we took is a qualitative example that indicates the roots being concentrated down the centre and along the bottom of the Hydrosac© although this choice of function can easily be refined later. The functional form we employed is

$$\frac{1}{\kappa(y,z)} = \begin{cases} 0 & \text{for} \quad z > f(y), \\ k_{\mathsf{min}} + (k_{\mathsf{max}} - k_{\mathsf{min}})\frac{h-z}{h} & \text{for} \quad z \le f(y), \end{cases} \tag{17}$$

where f is given by

$$f(y) = \frac{h(y - y_2)}{y_1 - y_2},$$

with $y_1 = 0.1$ and $y_2 = 0.2$, which indicates the location of the roots and k_{min}, k_{max} and they are given by the inverse of the permeability of the roots, at the top and bottom , respectively. We also take the viscosity to be: $\mu = 10^{-6}\,\mathrm{m^2\,s^{-1}}$ which is the viscosity of water at $18\,^\circ\mathrm{C}$.

We define a geometry within Mathematica that is representative of the actual geometry of a Hydrosac© and solve (14) and (15) numerically. We run this for a low and a high permeability taken to be: $\kappa_{max} = 1000$ and $\kappa_{max} = 0$, respectively. In each case, we take $k_{\mathsf{min}} = 0$. Our results are plotted in (12). They indicate that there is a large potential for stagnation within the Hydrosac© . In particular, the sharp corners of the Hydrosac© and along the bottom are areas where stagnation occurs. This model currently does not account for mixing due to bubbles. It is likely that the introduction of bubbles causes mixing in the centre of the bottom of the sac, however we would anticipate that bubbles may not avoid the problems with the sharp corners. A possible remedy for the difficulty would be to introduce additional walls to the Hydrosac© that round-off the corners.
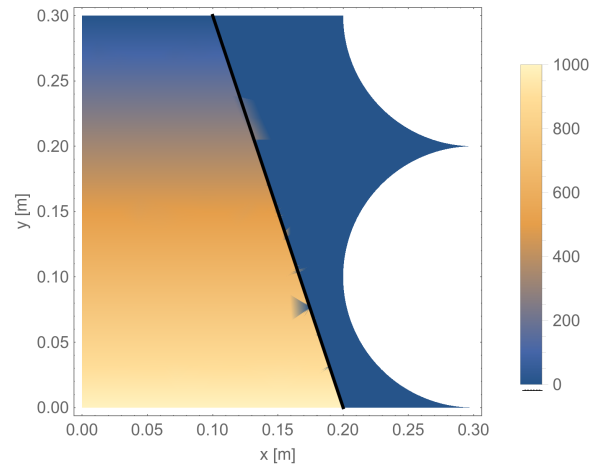
Figure 11: Example of the permeability field $1/\kappa$.
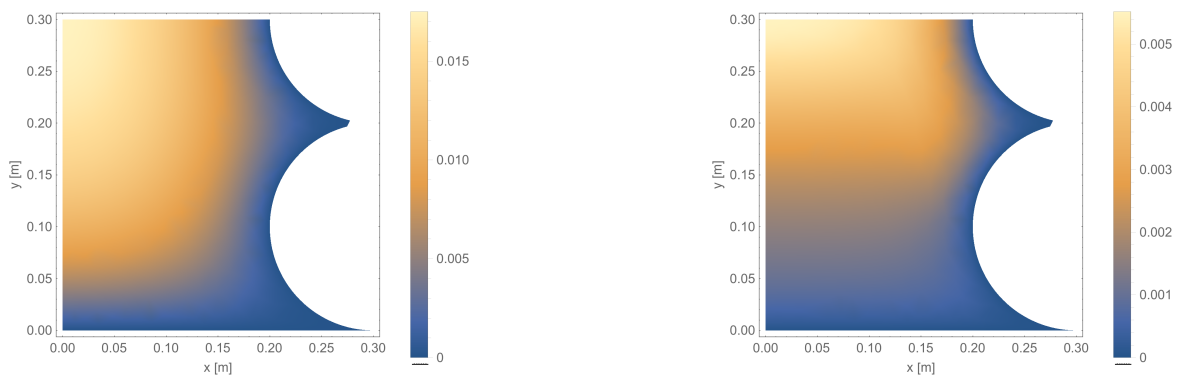
Figure 12: Out-of-plane velocity profiles of 2D model for high permeability (left) and low permeability (right).

7.1   Shear layer model

Before considering the mixing effects of bubble flow, let us first seek to explain one possible source of stagnation in the inlet flow. Since the Reynolds number for the meso-scale flow (without bubbles) is of the order $Re = \mathcal{O}(10^2)$, we expect a laminar regime. By assuming a simplified geometry, where the roots are represented by a porous cylinder, and we ignore the outer walls of the Hydrosac© (see Figure 13), we can make use of classic laminar solutions to describe our flow.

At the mesoscale, we represent the root system of a single plant as a porous cylinder. The plant roots provide a resistance to the flow that is sufficient to slow it down within the area beneath a single plant. In this way, as the flow passes through and around the root cylinder, we expect the streamwise velocity profile to have an approximately a "top-hat" profile. That is, slower flow in the cylinder region (with speed U_2) and faster flow (with speed U_1) in the outer regions that do not come into contact with the roots. See Figure 13. It is well known see e.g. [10], that such a discontinuous velocity profile is unstable to perturbations (due to the Kelvin-Helmholtz instability) and results in a laminar shear layer that grows between the fast and slow regions of flow. Here we make the key assumption that the speeds of the streams, U_1 and U_2, do not vary with longitudinal position x. This allows us to make use of the classic laminar shear layer solution for flow between unconfined parallel streams.

The classic laminar shear layer problem is described in detail by Schlichting [10], but here we give a brief outline.We assume that the flow is two-dimensional and symmetric about the centreline of the Hydrosac© . Therefore, we restrict attention to one half of the domain. We assume that a short distance downstream of the cylinder the velocity is given by the top hat profile

$$u = \begin{cases} U_1, & y > 0, \\ U_2, & y \leq 0, \end{cases} \tag{18}$$

where we have chosen our coordinate axes (x, y) such that the origin is located at the discontinuity in the velocity profile. For $x > 0$ a thin shear layer grows between the constant velocity streams. Since we have assumed constant U_1, U_2, we can take y varying between $-\infty$ and ∞ without loss of generality. We expect this to be a valid assumption until the point where the shear layer originating from one side of the cylinder interacts with the shear layer from the other side (which we discuss in more detail later). Therefore, if the cylinder has diameter D, we restrict our attention to regions of the flow where the shear layer is located within $y > -D/2$.

The shear layer is expected to occupy a thin region, in which the flow is well approximated

by the steady two-dimensional boundary layer equations

$$\frac{\partial u}{\partial x} + \frac{\partial v}{\partial y} = 0, \tag{19}$$

$$u\frac{\partial u}{\partial x} + v\frac{\partial u}{\partial y} = -\frac{1}{\rho}\frac{\partial p}{\partial x} + \nu\frac{\partial^2 u}{\partial y^2}, \tag{20}$$

$$0 = -\frac{1}{\rho}\frac{\partial p}{\partial y}. \tag{21}$$

Due to (21) and the fact that there is no pressure gradient at $y \to \infty$, the pressure is constant everywhere. Hence, by making the following transformation to similarity variables

$$\eta = y\sqrt{\frac{U_1}{\nu x}}, \tag{22}$$

$$u = U_1 f'(\eta), \tag{23}$$

$$v = \frac{1}{2}\sqrt{\frac{\nu U_1}{x}}(\eta f'(\eta) - f(\eta)), \tag{24}$$

the momentum equation (20) becomes

$$ff'' + 2f''' = 0, \tag{25}$$

which is often called the Blasius equation.

The appropriate boundary conditions for the streamwise velocity are

$$u \to U_1, \quad y \to \infty, \tag{26}$$

$$u \to U_2, \quad y \to -\infty. \tag{27}$$

From [11] there is also the boundary condition

$$v(x, \infty) = -\frac{U_2}{U_1}v(x, -\infty). \tag{28}$$

The condition (28) indicates that there is greater entrainment from the slower stream than the faster stream. Hence the dividing streamline, along which $v = 0$, is inclined downwards from the x-axis. This is in accordance with experimental observations [12].

In terms of the similarity variables, these boundary conditions become

$$f'(\infty) = 1, \tag{29}$$

$$f'(-\infty) = \lambda, \tag{30}$$

$$\lim_{\eta\to\infty}(\eta f'(\eta) - f(\eta)) = -\lambda \lim_{\eta\to-\infty}(\eta f'(\eta) - f(\eta)), \tag{31}$$

where $\lambda = U_2/U_1$ is the velocity ratio between slow and fast streams.

There is no known analytical solution to the system of equations (25), (29)-(31), but a numerical solution can be computed by approximating the domain as finite but large (e.g. $-100 < y <$
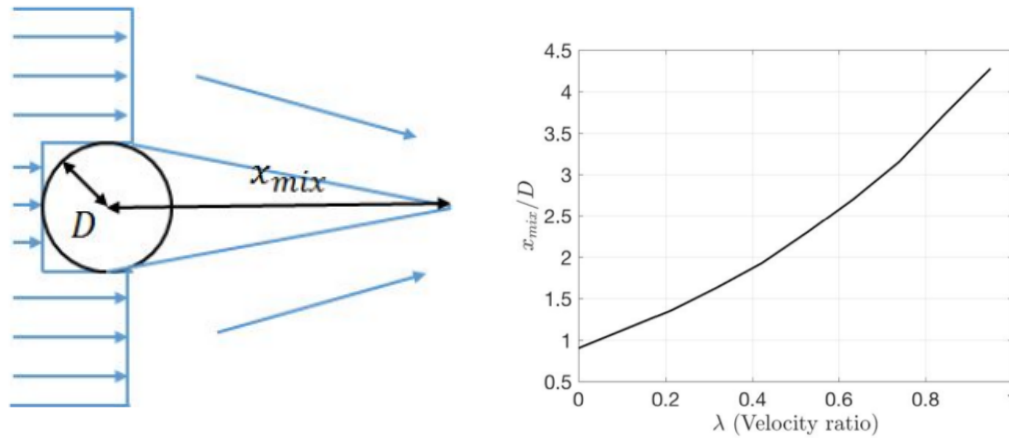
Figure 13: Shear layer model

100). The inner and outer boundaries of the shear layer are given by

$$y_{outer} = \eta_{outer}\sqrt{\frac{\nu x}{U_1}}, \tag{32}$$

$$y_{inner} = \eta_{inner}\sqrt{\frac{\nu x}{U_1}}, \tag{33}$$

where η_{outer} and η_{inner} are approximated as

$$f'(\eta_{outer}) = \lambda + 0.95(1 - \lambda), \tag{34}$$

$$f'(\eta_{inner}) = \lambda + 0.05(1 - \lambda). \tag{35}$$

Since the inner stream is relatively lacking in nutrients compared with the outer stream, it is important to understand where the inner boundary of the shear layer reaches the centre-line of the flow in the Hydrosac© . The flow upstream of this point consists of low-nutrient water, whereas the flow downstream is a mixture of low-nutrient and high-nutrient water. The place where the shear layer reaches the centreline is therefore a good approximation of the minimum recommended spacing between plants.

Therefore, if the diameter of the cylinder is D, then the distance for the inner region to disappear is given implicitly by the expression

$$y_{inner}(x_{mix}) = -\frac{D}{2}. \tag{36}$$

Since the solution to (25), (29)-(31) depends on the velocity ratio λ, so too does the distance x_{mix}.

In Figure 13 we plot the non-dimensional distance x_{mix}/D as a function of the parameter λ. We see that x_{mix}/D increases with λ. This is because larger values of λ produce a weaker shear layer which grows more slowly.

A simple experimental measurement of the velocity within the Hydrosac© could allow us to estimate the velocity ratio λ, and hence the appropriate spacing of the plants. In any case, these results suggest that the optimum spacing should be no less than around 4 cylinder diameters.

7.2 Bubble flow model

We have seen from the experiments in Sec. 4 that the longitudinal flow is turned off the majority of the time, and that the bubbles have a considerable effect on the mixing of the dye. We investigate the case in which there is no longitudinal flow and study the effect of bubbles in a cross section using a multiphase model. We assume that there are a large number of small bubbles so that we can approximate the bubbles by a continuum. Furthermore, we assume that the bubbles are in an equilibrium so that the buoyancy force acting on the bubbles balances with the drag force exerted on the bubbles by the fluid. Our model is summarised as follows:

$$\text{Conservation of air mass:} \quad \frac{\partial}{\partial t}(\alpha \rho_a) + \nabla \cdot (\alpha \rho_a \mathbf{u}_a + D\nabla(\alpha \rho_a)) = 0, \tag{37}$$

$$\text{Conservation of water mass:} \quad \frac{\partial}{\partial t}((1-\alpha)\rho_f) + \nabla \cdot ((1-\alpha)\rho_f \mathbf{u}_f) = 0, \tag{38}$$

$$\text{Conservation of water momentum:} \quad \frac{\mathrm{D}}{\mathrm{D}t}(1-\alpha)\rho_f \mathbf{u}_f = -\nabla p + \mu \nabla^2 \mathbf{u}_f - \frac{1}{\kappa}\mathbf{u}_f - \mathbf{F}_d, \tag{39}$$

$$\text{Bubble force balance:} \quad \mathbf{F}_d - \frac{4\pi}{3}a^3(\rho_f - \rho_a)\mathbf{g} = 0, \tag{40}$$

$$\text{Air volume fraction:} \quad \alpha = \frac{4\pi}{3}a^3 n. \tag{41}$$

Here α is the volume fraction of air, ρ_a is the density of air, ρ_f is the density of water, $\mathbf{u}_a$ is the velocity of air phase, D is the diffusivity of air bubbles in water, $\mathbf{u}_f$ is the velocity of the water, p is the pressure in the water, μ is the viscosity of water, κ is the root drag coefficient, $\mathbf{F}_d$ is the drag force acting on the bubble, a is the radius of the bubbles, $\mathbf{g}$ is the gravitational acceleration and n is the number of bubbles per unit volume of fluid.

We need boundary conditions for eqs. (37) to (39) to have a well posed system. There are three cases that we need to consider, the free surface of the fluid, the wall of the Hydrosac© and the bubble source. On each of the boundaries we use no flux conditions for the conservation of water and air mass.

$$\mathbf{u}_f = 0 \quad \text{and} \quad \mathbf{n} \cdot N_{\alpha \rho_a} = 0,$$

where $\mathbf{n}$ is the normal vector of the surface and $N_{\alpha \rho_a}$ is the flux of air mass through the boundary. Furthermore we need to have a source of bubbles in the system, this can be done by using a volume source of bubbles in the place where the pipe that is the bubble source would be.

Time=10 s   Surface: Velocity magnitude, liquid phase (m/s)
Streamline: Velocity field, liquid phase
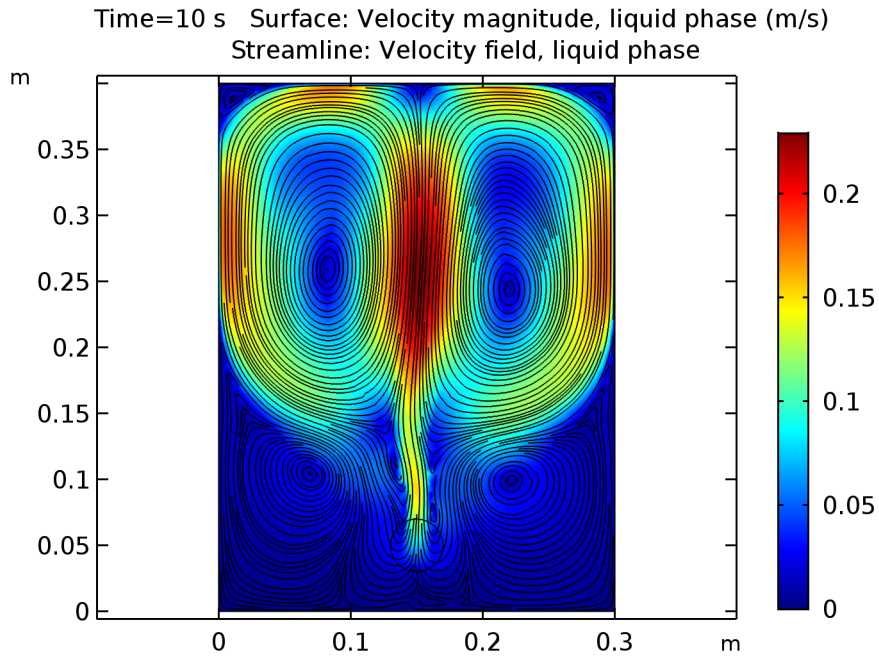
Figure 14: Velocity field induced by bubbles in a simplified geometry calculated by `COMSOL` for the model presented from eq. (37) to eq. (40).

This model is inbuilt within `COMSOL` using research from e.g. [13], thus can be solved for an arbitrary geometry. We use a simplified geometry to get an order of magnitude estimate for the recirculation speed.

By computing the solution of eqs. (37) to (41) in `COMSOL`, we find that the bubbles generate recirculation of water in the cross section that we would expect intuitively. The results are shown in fig. 14.

Using this model could give us more information about the placement of the bubble sources and the relationship between the bubble size and the generated flow, but to get reliable results we would need more information about the material parameters that occur in the model, for example: D the diffusivity of bubbles in water and κ the drag coefficient on the roots are two parameters that we do not know accurately, hence the numerical results are only qualitative.

Nevertheless, we can estimate the recirculation speed. Using the properties of water for the fluid, air for the dispersed gas bubbles, assuming $0.1\,\mathrm{kg\,m^{-3}}$ gas flow from the pipe and assuming $1\,\mathrm{mm}$ bubble size, the recirculation speed is of the order $0.2\,\mathrm{m\,s^{-1}}$. This suggests that within the $T_a = 1$ min that the bubble flow is on there will be muliple, $\mathcal{O}(20)$, circuits of fluid motion within a cross-section containing a plant. This is likely to be more than sufficient to enable effective nutrient mixing.

8 Conclusion

8.1 Key findings

1. We have analysed a range of reduced-order fluid dynamic models of the spread of nutrients within the Phytoponics Hydrosac© system that was in place for the Aberystwyth trials in Summer 2018.

2. The modelled Hydrosac© allows for the infiltration and mixing of nutrients by a combination of two processes that are repeated periodically; inlet flow and mixing due to bubble flow.

3. Nutrients enter the flow as the bag is being filled from the inlet. This causes a convection of nutrients throughout the bag from the inlet end towards the drain. Both experimental and modelling evidence suggest Several cycles of the inlet flow are required for the nutrients to reach the far end of the bag.

4. The inlet flow alone does not allow mixing of nutrients into the plant root systems, with the main flux of nutrients being confined to regions of high permeability (low root density). In particular there are near stagnation zones in the regions around each plant root system, with re-mixing of nutrients into the centreline of the channel only predicted to occur after 4 plant diameters, which is a greater separation than used in the current Hydrosac© .

5. Both experimental evidence and that from the literature suggests that the inflow of fine air bubbles is sufficient to drive recirculation within each cross-section of the sack. Computational modelling of simplified two-phase flow agrees with this finding and suggests that the recirculation is sufficient to cause significant mixing of nutrients from the stagnant zones into the plant root system.

6. Nevertheless some stagnant regions are likely to remain in the bottom corners of the Hydrosac© .

7. Nutrient diffusion, the flow from drippers placed above each pot and any wave or sloshing effects can generally be ignored as they do not contribute significantly to the nutrient mixing.

8. We have not specifically modelled the flux of pathogens or waste products, other than to implicitly assume that this mirrors the flux of nutrients through the bag.

9. Nor have we specifically modelled the aeration of water, other than the effect of the bubbles on inducing fluid mixing. Nor has this study modelled the uptake of oxygen by the plant roots.

10. The overall conclusion is that a combination of inflow and bubble flow is necessary in order to provide good nutrient mixing.

11. Moreover, the approach used is sufficient to gain quantitative accuracy and therefore can be used to optimise the operation of the existing Hydrosac© or future generations that Phytoponics may develop.

8.2 Recommendations

Recommendation 1. We recommend that a full hybrid model be developed along the lines developed here. In particular, the homogenisation process in Sec. 6.1 should be completed and fed with more realistic numbers arising from properties of the roots. Also the computational model in Sec. 7 should be fully parametrised. Given the brief time in which the bubble flow is on compared to the whole cycle $T_a/T_2 = 1/15$, the final state of mixing after the bubble flow can be fed back into the macroscopic flow model for the rest of the cycle. Thus, the two models are run separately.

Recommendation 2. The combined model should be used to optimise the dynamic parameters of the operation of the Hydrosac© . In particular, by understanding the dependence of the distribution of nutrient concentration throughout the sack on the control parameters $T_1, T_2, T_{\mathrm{on}}, T_a, w_{\max}, w_{\min}$ etc., minimisation of energy input can be sought.

Recommendation 3. The model so-far suggests that regions of stagnation, and hence poor mixing, may still exist in the Hydrosac© near sharp corners where the air bags join each other and join the bottom of the sack. We recommend that future designs of the sack try to avoid any sharp corners.

Recommendation 4. We recommend that the model be extended to include both levels of dissolved oxygen (building on the report [2]) and waste. Efficient operation of the Hydrosac© can be

Recommendation 5. More effort should be put into establishing accurate parameters, for example for effective permeabilities, nutrient and oxygen uptake by roots, and on the properties of waste products.

Recommendation 6. For future trials, further quantitative experiments should be planned in which dynamic measurements are taken at multiple points within the Hydrosac© on nutrient and dissolved oxygen levels. These measurements should be used to parametrise, validate and verify the model.

Recommendation 7. Finally, we recommend a plant growth and fruiting model can be established as a function of different levels of nutrient and oxygen, plant spacing etc. to produce information on yield as a function of energy input.

References

[1] A. Champneys, W. Lee, A. Leida, I. Hewitt, M. Mcphail, E. Murphy, J. Ockendon, L. Parkin, and L. Roberts. Optimising the design of polythene hydroponics beds, 2017. Report of Agri-Food Study Group with Industry, Bath.

[2] A. Champneys, R. Dyson, A. Dixon, A. Lacey, K. Newmann, L. Parkin, and M. Ptashnyk. Understanding and manipulating aeration dynamics affecting dissolved oxygen in hydroponic system, 2018. Report of Agri-Food Study Group with Industry, Edinburgh.

[3] A. Wüest, N.H. Brooks, and D.M. Imboden. Bubble plume modeling for lake restoration. *Water Resources Research*, 28(12):3235–3250, 1992.

[4] T. Asaeda and J. Imberger. Structure of bubble plumes in linearly stratified environments. *Journal of Fluid Mechanics*, 249:35–57, 1993.

[5] F. Risso. Agitation, mixing, and transfers induced by bubbles. *Annual Review of Fluid Mechanics*, 50:25–48, 2018.

[6] J.J. Ulbrecht and Z. Sema Baykara. Significance of the central plume velocity for the correlation of liquid phase mixing in bubble columns. *Chemical Engineering Communications*, 10(1-3):165–185, 1981.

[7] L.F. Burns and R.G. Rice. Circulation in bubble columns. *AIChE journal*, 43(6):1390–1402, 1997.

[8] S. Dalziel, 2018. Personal communication.

[9] G. Allaire. Homogenization of the navier-stokes equations in open sets perforated with tiny holes i. abstract framework, a volume distribution of holes. *Archive for Rational Mechanics and Analysis*, 113(3):209–259, Sep 1991.

[10] H. Schlichting and K. Gersten. *Boundary-layer theory*. Springer, 2016.

[11] L. Ting. On the mixing of two parallel streams. *Studies in Applied Mathematics*, 38(1-4): 153–165, 1959.

[12] S.B. Pope. *Turbulent flows*. Cambridge University Press, 2000.

[13] A. Sokolichin, G. Eigenberger, and A. Lapin. Simulation of buoyancy driven bubbly flow: established simplifications and open questions. *AIChE Journal*, 50(1):24–45, 2004.